

2007 April 3

Imaging the Ionized Disk of the High-Mass Protostar Orion–I

M. J. Reid

Harvard-Smithsonian Center for Astrophysics, 60 Garden Street, Cambridge, MA 02138

reid@cfa.harvard.edu

K. M. Menten

Max-Planck-Institut für Radioastronomie, Auf dem Hügel 69, D-53121 Bonn, Germany

kmenten@mpifr-bonn.mpg.de

L. J. Greenhill

Harvard-Smithsonian Center for Astrophysics, 60 Garden Street, Cambridge, MA 02138

lgreenhill@cfa.harvard.edu

C. J. Chandler

National Radio Astronomy Observatory, P.O. Box 0, Socorro, NM 87801

cchandle@nrao.edu

ABSTRACT

We have imaged the enigmatic radio source-I (Orion–I) in the Orion-KL nebula with the VLA at 43 GHz with 34 mas angular resolution. The continuum emission is highly elongated and is consistent with that expected from a nearly edge-on disk. The high brightness and lack of strong molecular lines from Orion–I can be used to argue against emission from dust. Collisional ionization and H⁺ free-free opacity, as in Mira variables, require a central star with $\gtrsim 10^5 L_{\odot}$, which is greater than infrared observations allow. However, if significant local heating associated with accretion occurs, lower total luminosities are possible. Alternatively, photo-ionization from an early B-type star and p⁺/e[−] bremsstrahlung can explain our observations, and Orion–I may be an example of ionized accretion disk surrounding a forming massive star. Such accretion disks may not be able to form planets efficiently.

Subject headings: infrared: stars — ISM: individual (Orion Kleinmann-Low) — stars: individual (I,IRc 2) — stars: formation — planetary systems: formation

1. Introduction

The nearest massive star forming region, the Kleinmann-Low (KL) nebula in the Orion molecular cloud, is at a distance 480 pc (Genzel et al. 1981). While the brightest near-infrared source in Orion-KL (Kleinmann & Low 1967) is the Becklin-Neugebauer (BN) object, it contributes only a small fraction of the total nebular luminosity of $\sim 10^5 L_{\odot}$ (see Thronson et al. 1986 and references therein). Other young stellar objects (YSOs) are deeply embedded and hidden from view at infrared (IR) wavelengths. An object giving rise to strong mid-IR emission, IRc 2, has been long suspected to be the dominant energy source in Orion-KL (Downes et al. 1981; Genzel et al. 1981; Shuping, Morris & Bally 2004), but hidden by > 60 mag of visual extinction (Gezari, Backman & Werner 1998; Greenhill et al. 2004b). However, IRc 2 breaks-up into several compact regions (Dougados et al. 1993; Greenhill et al. 2004b). Moreover, Gezari (1992) and Menten & Reid (1995) showed that IRc 2 is offset from the compact radio source-I (hereafter Orion-I), and some components of IRc 2 could arise from reflected light. Orion-I is very deeply embedded and Greenhill et al. (2004b) estimate optical depths > 300 at 8 and 22 μm wavelengths.

The radio source Orion-I is an enigmatic object. Proper motion measurements suggest that Orion-I might have been part of a multiple system that disintegrated ≈ 500 years ago (Gómez et al. 2005). Strong H_2O and OH (Cohen et al. 2006) masers are concentrated near Orion-I, and the H_2O masers are distributed in an elongated pattern along position angle (PA) $\approx 45^\circ$ (East of North). The H_2O masers seem to be expanding about a central position in the general vicinity of Orion-I (Genzel et al. 1981). Orion-I also displays strong SiO masers, which are usually associated with evolved asymptotic giant branch (AGB) or supergiant stars and are very rare in star forming regions (Hasegawa et al. 1985). Interferometric maps of the SiO masers with the BIMA array at an angular resolution of $\approx 1''$ indicated the possibility that they came from a rotating and expanding disk (Plambeck et al. 1995). Higher resolution observations with the VLA (Menten & Reid 1995) located Orion-I at the center of the SiO masers. Menten & Reid argued that the presence of vibrationally-excited SiO masers, which require temperatures exceeding 1000 K (e.g., Lockett & Elitzur 1992) at a radius of ≈ 50 AU from Orion-I, was strong evidence that it must be a very luminous object ($\sim 10^5 L_{\odot}$).

Observations by Greenhill et al. (1998) with the VLBA at a resolution of ~ 1 mas clearly resolved the SiO masers into four “arms” that together make an $0.2''$ “X”-like pattern. Since an X-like pattern has two symmetry axes, two models for the SiO masers have been forwarded. The SiO masers could form in the limbs of a high velocity bi-conical outflow projected along a NW–SE axis (Greenhill et al. 1998; Doeleman, Lonsdale & Pelkey 1999). In this model, the western (eastern) arms are moving away from (toward) the observer and

hence are red-shifted (blue-shifted) with respect to the systemic velocity. Alternatively, the SiO masers could form in material being expelled from a rotating disk, whose spin axis is projected NE–SW. In this model, the western (eastern) arms are moving away from (toward) the observer owing to rotation (Greenhill et al. 2004a). As discussed in §3, evidence favors the latter model of a rotating, nearly edge-on, disk centered on Orion–I.

We have used the VLA at 43 GHz and imaged the radio continuum emission associated with Orion–I and located it precisely toward the center of the SiO maser X-like pattern. These data together give the clearest picture yet presented of the nature of a high-mass, YSO, disk on scales of ≈ 16 AU. In this paper we concentrate on understanding the properties and nature of the continuum emission from the disk-like structure of Orion–I.

2. Observations & Results

Our observations were made on 2000 November 10 with the NRAO¹ Very Large Array (VLA) in a manner similar to those of Menten & Reid (1995). All 27 antennas had 40–50 GHz receivers, compared to our previous observations with only 9 antennas. The recently installed receivers had better noise performance than the ones available in 1994 and were placed on antennas providing longer interferometer baselines. Thus, the present data yielded lower noise levels and higher angular resolution compared to our previous data.

In order to image the continuum emission from Orion–I and to locate this emission with respect to the SiO masers, we employed a dual-band continuum setup with a narrow band (1.56 MHz), covering red-shifted SiO $v=1$, $J=1-0$ masers between LSR velocities of $10.8 - 21.3 \text{ km s}^{-1}$ (assuming a rest frequency of 43122.08 MHz), and a broad band (50 MHz), centered at 43164.9 MHz on a line-free portion of the spectrum. Both frequency bands were observed in dual-circular polarizations. We observed from 0^h30^m to 10^h30^m local sidereal time. Absolute flux density calibration was obtained from an observation of 3C286, assuming the flux density spectrum of Baars et al. (1977). Observations of the quasar 0501–019, measured to be 0.74 Jy, were interspersed with Orion–I to monitor gain variations and to determine electronic phase-offsets between the bands.

The narrow-band data were then “self-calibrated” with the very strong maser signal as a phase reference. The phase and amplitude corrections were then applied to the broad-band data, and a high quality map of the continuum emission was produced. A detailed

¹The National Radio Astronomy Observatory (NRAO) is operated by Associated Universities, Inc., under a cooperative agreement with the National Science Foundation.

description of this cross-calibration procedure can be found in Reid & Menten (1997). Once the continuum signals were “cross-self-calibrated” with the SiO maser signals, the data were imaged with the Astronomical Image Processing System (AIPS) task IMAGR. We produced maps with two different weightings of the (u,v)-data, shown in Fig. 1. Using IMAGR weighting parameter “ROBUST=5” the dirty beam was 58×45 mas at a PA of -20° , and we restored the image with a round beam of 50 mas (approximately the geometric-mean size). Using “ROBUST=0” the dirty beam was 41×28 mas at PA of -30° , and we restored the image with a round beam of 34 mas. At a distance of 480 pc, 34 mas corresponds to 16 AU. These maps had rms noise levels of $0.13 \text{ mJy beam}^{-1}$ and $0.14 \text{ mJy beam}^{-1}$, respectively.

In order to image the SiO maser emission at high spectral resolution, several scans in spectral-line mode were interspersed with the dual-band continuum observations. We covered all of the SiO maser emission with a bandwidth of 6.25 MHz and 128 spectral channels, which provided a velocity resolution of 0.34 km s^{-1} . The line data were self-calibrated by choosing a channel with strong emission as a reference, and the resulting phase and amplitude corrections were applied to the other channels. Scans of the strong extragalactic continuum sources 3C 84 and 3C 273 provided bandpass calibration. We produced a spectral-line data cube, which we restored with a 30 mas beam, taking advantage of the high signal-to-noise ratio and slightly “over-resolving” the dirty beam of 43×27 mas.

Alignment of the continuum and maser emission to about 5 mas accuracy was achieved by producing a pseudo-continuum map from the line data, using spectral channels covering the velocities that were within the 1.56 MHz passband of the dual-band continuum setup, and comparing it with the maps obtained from the dual-band data. Based on this cross-registration, we show SiO maser maps, smoothed to 5.43 km s^{-1} resolution, superposed on the continuum emission of Orion-I in Fig. 2. This figure shows that the continuum emission is precisely centered among the four SiO maser arms, whose innermost ends nestle tightly against the disk-like continuum structure.

3. Results & Discussion

Our images of the continuum emission from Orion-I at 43 GHz are shown in Fig. 1. The top and middle panels of the figure are maps made with resolutions of 50 and 34 mas, respectively. The total flux density of Orion-I is 13 mJy and the peak brightness at 34 mas resolution is $3.0 \text{ mJy beam}^{-1}$. The emission appears to be composed of a compact component, near the center of the source, and a component elongated NW–SE. Assuming the elongated component is approximately uniformly bright, it would contribute about $0.8 \text{ mJy beam}^{-1}$ at the center of the source, leaving 2.2 mJy for the compact component. Subtracting a 0.8 mJy

point-source centered at the position of peak brightness, we obtain the image shown in the bottom panel of Fig. 1. This reveals a disk-like feature with a radius of ≈ 35 AU and a brightness of about 1 mJy beam^{-1} . Away from the center of the source, the true brightness is a lower limit, since the feature is not well resolved perpendicular to its elongation. We also note that the peak brightness along the disk-like feature does not follow a straight line on the sky. Instead, it appears to bend as might be expected from a warped disk.

In the following discussion, we assume that the compact emission comes from the immediate environment of a YSO, and that the elongated component traces a nearly edge-on disk, whose spin axis is aligned northeast–southwest. Briefly, the evidence supporting this model is as follows. Greenhill et al. (2004a) report detection of a curved arc of SiO maser emission bridging the gap between the base of the south and west arms. Evidence of this emission can also be seen in the -3.47 and 12.8 km s^{-1} channel maps (Fig. 2). The bridge emission displays a radial velocity gradient, and some features have tangential proper motions, consistent with material rotating close to the nearside of a disk. Such emission is not anticipated for a bipolar outflow. Additionally, Greenhill et al. (2004a) note that H_2O maser emission comes from “caps” displaced predominantly $0''.2$ – $0''.7$ toward the northeast and southwest of Orion–I, i.e., along the disk spin axis. These caps show outward motion and indications of rotation; the red- and blue-shifted emission tend to lie on opposite sides of the spin axis, consistent with the inferred direction of disk rotation. A more complete presentation of these findings will appear in Greenhill et al. (2007).

At the center of the disk, the source appears slightly extended perpendicular to its elongation (i.e., along $\text{PA} = +45^\circ$). It is possible that a weak jet emanates from the YSO, perpendicular to the disk, resulting in the extended appearance at the center. Clearly, higher sensitivity observations are needed to understand this structure.

What are the physical conditions in the Orion–I source? To answer this question, one must know the emission mechanism (opacity source) for the cm-wave photons. The cm-to-mm wavelength spectrum of the entire source can be characterized as a power law with flux density, S_ν , rising with observing frequency, ν , as $S_\nu \propto \nu^{1.6}$ (Menten & Reid 1995; Beuther et al. 2006), approaching that of a black body. Since the source is not well resolved spatially at lower frequencies with the VLA, the spectral index does not allow us to discriminate between an inhomogeneous, single-component model (where the spectral index is shallower than 2.0, because unity optical-depth occurs at a smaller radius at higher frequencies) and a two-component model (with an optically thick central component and a partially optically thin disk-like structure).

We think it unlikely that dust emission could be a dominant contributor to the cm- to mm-wavelength emission of Orion–I. A dense, warm, dusty disk would be expected to show

a plethora of molecular lines at mm/sub-mm wavelengths. While Beuther et al. (2006) find numerous, strong, molecular lines toward the nearby “hot core,” they find no strong lines toward the position of Orion–I (only weak SO lines and, of course, the strong SiO masers slightly offset from Orion–I). Thus, we look to other emission mechanisms to explain both the YSO peak and the elongated disk components.

The observations could be modeled with gas at ≈ 8000 K, where hydrogen is fully ionized (proton-electron bremsstrahlung). In this case, the data require an optically thick central component and a partially optically thin disk component. Alternatively, the emission could be partially optically-thick from gas at < 5000 K, where hydrogen is predominantly neutral and free electrons come from low ionization-potential metals (H-minus free-free). The latter case applies in the “radio photospheres” of Mira variables at roughly 2 stellar radii (Reid & Menten 1997). In the following subsections, we present two classes of models for the Orion–I cm-wave emission. These models are exploratory and designed only to elucidate characteristic physical conditions.

3.1. Collisional Ionization: H[−] free-free Opacity

In several ways Orion–I appears similar to a Mira-like variable star. Such stars display OH, H₂O, and SiO masers, as seen in Orion–I. In addition, Mira variables have continuum emission detectable with the VLA at cm wavelengths, with brightness temperatures of ≈ 1600 K (Reid & Menten 1997). The radio continuum of Mira variables occurs in an optically-thick (spectral index ≈ 1.9) “radio photosphere” with characteristic temperature of ≈ 1600 K and density of $\sim 10^{12}$ cm^{−3}. Under these conditions the dominant opacity source is H-minus free-free interactions, coming from free electrons interacting with neutral hydrogen (either atomic or molecular). This is analogous to normal proton-electron bremsstrahlung, except that the interaction is about 10^4 weaker (Dalgarno & Lane 1966), requiring correspondingly higher densities. At these temperatures and densities, sufficient free electrons can be created by collisional ionization of Na and K (Reid & Menten 1997).

The SiO $v=1$, $J=1-0$ maser emission at 43 GHz originates from the first vibrationally-excited state at ≈ 1800 K above the ground-state, and models of maser pumping require temperatures of ≈ 1200 K and hydrogen densities of $\sim 10^{9-10}$ cm^{−3} for strong maser action (Alcolea, Bujarrabal & Gallego 1989; Lockett & Elitzur 1992; Bujarrabal 1994). Since the continuum emission region is more compact and has a higher (brightness) temperature than required for SiO maser excitation, finding the loci of SiO maser emission extending outward from the continuum, as shown in Fig. 2, is reasonable and as observed for Mira-like variables (Reid & Menten 2003). As both Miras and Orion–I display similar cm-to-mm wavelength

spectral indexes and have a similar configuration of continuum and maser emission, there is circumstantial evidence for similar physical conditions and mechanisms.

We have explored models for the disk-like emission of Source-I owing to H^- free-free opacity. Assuming conditions similar to a Mira-like radio photosphere, material at density $\sim 10^{11} \text{ cm}^{-3}$ and temperature $\approx 1500 \text{ K}$ requires a path length of $\approx 2 \text{ AU}$ in order to achieve an optical depth of ≈ 0.5 (Reid & Menten 1997), possibly explaining the observed disk brightness temperature of $\gtrsim 450 \text{ K}$. This path length is about 10% of the disk radius and, thus, is easily achievable. Such a model has the benefit that a single power-law can explain the observed spectral energy distribution for the entire Orion-I source between 8 and 350 GHz. However, recently Beuther et al. (2006) have measured the flux density of Orion-I at 690 GHz to be between 3.5 and 9.9 Jy. Since the extrapolation of the cm-wave continuum spectrum to 690 GHz predicts under 2 Jy, an additional component (e.g., dust on a scale of $0.2''$ to $2''$) seems required to explain the sub-mm wavelength spectrum of Orion-I, making a single emission mechanism unlikely.

For Orion-I, we observe a disk-like component that extends to about $0.08''$ ($\approx 40 \text{ AU}$) from the star. We have attempted to model the brightness profile of such a disk in a manner similar to that done for the radio photospheres of Miras (Reid & Menten 1997), but with a disk geometry. Specifically, we assume an edge-on disk that is centrally heated and is optically thick to most of the radiation from the YSO. In Fig. 3 we plot the observed brightness temperature in the map with 34 mas resolution (middle panel of Fig. 1) as a function of position along the disk elongation. The physical parameters of the central star and disk are listed in Table 1 for model A. In Fig. 3 we overplot the model brightness (blue dotted line) convolved with the observed restoring beam. While model A provides a reasonable fit to the observations, the model requires the central star to have a total luminosity of $\sim 3 \times 10^5 L_\odot$ and a disk mass of $\sim 3 M_\odot$. These are general characteristics of this class of models and are not sensitive to details of the parameters. Note that a similarly large luminosity may also be required to explain the SiO masers (Menten & Reid 1995). Reducing the stellar luminosity requires substantially increasing the disk mass (in order to increase opacity and maintain a high disk brightness temperature). Thus, such a model requires a fairly massive disk and a luminosity exceeding that from the IRc 2 region (Gezari, Backman & Werner 1998; Greenhill et al. 2004b) and, perhaps, even that of the entire Orion-KL nebula (Thronson et al. 1986). Since other energetic sources exist nearby (e.g., Source-n), we conclude that the disk component of Orion-I probably is not thermally (collisionally) excited by a central source.

While central heating of the disk component (and also the SiO masers) may be ruled out on energetic grounds, the material in the disk and the SiO masers may be partially locally

heated by accretion processes. Dissipation of energy in the disk could raise the temperature above that allowed by radiative equilibrium with the central star. Since the volume of the disk can be considerably less than that of a sphere of the same radius, increasing the disk temperature in this manner can require less total energy than for central heating alone. Thus, we evaluated models that allowed the disk temperature to fall with radius, r , more slowly than $r^{-1/2}$. One such model, described in Table 1 as model B and shown in Fig. 3, fits the data well and requires a central star luminosity of $5 \times 10^4 L_\odot$, comfortably below the observational limits.

As pointed out by Menten & Reid (1995), the SiO maser excitation also requires a very high luminosity source, were it to be centrally heated (i.e., assuming radiative equilibrium: $L = \sigma T^4 4\pi r^2$). However, infalling material might interact with outflowing material (and possibly magnetic fields) in the conical walls of a bi-polar outflow. This may add heat, augmenting the central source and providing the necessary high temperatures (≈ 1200 K) for strong SiO maser emission.

3.2. Photo-ionization: p^+/e^- Bremsstrahlung

Given the high luminosities and disk masses characteristic of models involving thermal ionization and H^- free-free opacity, we now consider a hotter central star. The observed brightness can be modeled with an early B-type star, which photo-ionizes a moderate density plasma. Indeed, since proton-electron bremsstrahlung is $\sim 10^4$ times stronger than H^- free-free per interaction, the disk plasma need only have a density $\sim 10^{-4}$ times lower.

Assume that Orion-I contains a hot central star and a photo-ionized disk (or a photo-ionized surface layer). The disk may contain a neutral central layer, which provides a reservoir for material that can be photo-ionized by the YSO (Hollenbach et al. 1994). The sub-mm wave spectrum of Orion-I, measured by Beuther et al. (2006), suggests a dust component dominates above 300 GHz, leaving a bremsstrahlung spectrum that becomes optically thin above ≈ 100 GHz. Such a turnover frequency can come from an electron density of $\sim 10^7 \text{ cm}^{-3}$ over a path length of 35 AU, comparable to the observed radius. These parameters yield an excitation parameter, U , of $\sim 10 \text{ pc cm}^{-2}$, which could come from a ZAMS B0–B1 star (Panagia 1973) of $\approx 10 M_\odot$ and a luminosity approaching $10^4 L_\odot$. A star of $\gtrsim 6 M_\odot$ is consistent with the rotation and expansion seen in VLBA maps of the SiO masers (Greenhill et al. 2004a; Cunningham, Frank & Hartmann 2005).

In Fig. 3 (dashed green line), we present a simple model of a brightness temperature profile along an edge-on, photo-ionized disk with a constant temperature. The physical pa-

rameters of the star and disk are given in the Table 1 as model C. This model provides a reasonable fit to the data, demonstrating that a photo-ionized disk can explain our observations.

Recently, Keto (2002, 2003) and Keto & Wood (2006) have shown that the inner portion of a disk can be fully ionized and still allow for continued accretion onto a massive protostar. They point out that inside a critical radius $r_c = GM/2c_s^2$, where G is the gravitational constant, M is the mass of the central protostar, and c_s is the sound speed in the (neutral or ionized) material, the protostar’s gravity exceeds the thermal pressure. For the stellar parameters given above for a ZAMS B0–B1 star, ionized accretion can proceed inside of the critical radius of about 25 AU. This critical radius is similar to the 35 AU radius of the disk observed at 43 GHz in Orion–I.

Keto (2007) explored models of ionized accretion in the presence of significant angular momentum. The example shown in the *right-hand* panel of his Fig. 1 corresponds to a star of $20 M_\odot$, an ionizing flux of 3×10^{46} photons s^{-1} (approximately a B0 – 09.5 star), and accreting material with specific angular momentum of $0.16 \text{ km s}^{-1} \text{ pc}$. The resulting critical radius for accretion of ionized gas is 54 AU. Scaling this to a $10 M_\odot$ star gives a critical radius of 27 AU, reasonably consistent with our observations.

An ionized accretion disk offers a natural explanation for the dearth of sub-mm wavelength spectral-lines, observed by Beuther et al. (2006) toward Orion–I, that would otherwise be expected for a dense and warm neutral disk. Thus, Orion–I may be a good example of a massive YSO accreting material after ionizing its inner accretion disk. If the disk is maintained at a temperature greater than $\approx 1500 \text{ K}$ out to a radius of 35 AU, as we observe in Orion–I, this may preclude planetary formation. Planet formation is thought to occur on a much longer time scale than the formation of a massive star. In order to form planets around massive stars, the early phases of planetesimal formation would have to overcome temperatures high enough to sublimate dust, and certainly not conducive to rapid grain growth. This difficulty is in addition to the well known problem of the short timescales for the formation of massive stars and dispersal of their disks.

4. Other High-mass Protostars

While Orion–I is probably the nearest high-mass protostellar object, more distant candidates include CRL 2136, W 33, AFGL 2591, and NGC 7538/IRS 9. These objects display cm-to-mm wavelength spectra closely resembling that of Orion–I, and whose continuum emissions are unresolved (or only marginally resolved) at 40 mas resolution (Menten & van der Tak

2004; van der Tak & Menten 2005). While none of these candidates have been observed to have SiO maser emission, Menten & van der Tak (2004) find that CRL 2136 has H₂O masers very close (in projection) to the continuum emission; the masers might arise in dense, hot gas following an accretion shock.

5. Future Observations

Our current image of Orion–I, at a resolution of 34 mas (≈ 16 AU), appears to show an ionized disk around a massive YSO. While this may be the best image to date of such a disk, our data are limited both in sensitivity and angular resolution. We have only about five resolution elements along the disk, and we have not clearly resolved the emission perpendicular to the disk. In order to improve significantly the sensitivity, of this image, we probably must await the completion of the EVLA phase-I project. Improved angular resolution, with the required higher sensitivity, could be achieved with the planned increase in baseline length of the EVLA phase-II or, in the long-term, with the Square Kilometer Array.

We thank L. Matthews for suggestions to improve the manuscript.

REFERENCES

- Alcolea, J., Bujarrabal, V. & Gallego, J. D. 1989, A&AS, 211, 187
- Baars, J. W. M., Genzel, R., Pauliny-Toth, I. I. K & Witzel, A. 1977, A&AS, 61, 99
- Beuther, H. et al. 2006, ApJ, 636, 323
- Bujarrabal, V. 1994, A&AS, 285, 953
- Cohen, R. J., Gasprong, N., Meaburn, J. & Graham, M. F. 2006, MNRAS, 367, 541
- Cunningham, A., Frank, A. & Hartmann, L. 2005, ApJ, 631, 1010
- Dalgarno, A. & Lane, N. F. 1966, ApJ, 145, 623
- Dougados, C, Léna, P., Ridgway, S. T., Christou, J. C. & Probst, R. G. 1993, ApJ, 406, 112
- Doeleman, S. S., Lonsdale, C. J. & Pelkey, S. 1999, ApJ, 510, L55
- Downes, D., Genzel, R., Becklin, E. E. & Wynn-Williams, G. C. 1981, ApJ, 244, 869

- Genzel, R., Reid, M. J., Moran, J. M. & Downes, D. 1981, *ApJ*, 244, 884
- Gezari, D. Y. 1992, *ApJ*, 396, L43
- Gezari, D. Y., Backman, D. E. & Werner, M. W. 1998, *ApJ*, 509, 283
- Gómez, L., Rodríguez, L. F., Loinard, L., Lizano, S., Poveda, A. & Allen, C. 2005, *ApJ*, 635, 1166
- Greenhill, L. J., Gwinn, C. R., Schwartz, C., Moran, J. M. & Diamond, P. J. 1998, *Nature*, 416, 59
- Greenhill, L. J., Chandler, C. J., Reid, M. J., Diamond, P. J. & Moran, J. M. 2004a, in “Star Formation at High Angular Resolution,” *Proceedings of IAU Symposium 221*, eds. M. G. Burton, R. Jayawardhana & T. L. Bourke, (San Francisco: ASP), p. 155
- Greenhill, L. J., Gezari, D. Y., Danchi, W. C., Najita, J., Monnier, J. D. & Tuthill, P. G. 2004b, *ApJ*, 605, L57
- Greenhill, L. J., Chandler, C. J., Reid, M. J., Diamond, P. J. & Moran, J. M. 2007, in preparation
- Hasegawa, T. et al. 1985, in “Masers, Molecules and Mass Outflows in Star Forming Regions,” ed. A. Haschick (Haystack Obs., Westford, MA), p. 275
- Hollenbach, D., Johnstone, D., Lizano, S. & Shu, F. 1994, *ApJ*, 428, 654
- Keto, E. 2002, *ApJ*, 580, 980
- Keto, E. 2003, *ApJ*, 599, 1196
- Keto, E. 2007, submitted to *ApJ*
- Keto, E. & Wood, K. 2006, *ApJ*, 637, 850
- Kleinmann, D. E. & Low, F. J. 1967, *ApJ*, 149, L1
- Lockett, P. & Elitzur, M. 1992, *ApJ*, 399, 704
- Menten, K. M. & Reid, M. J. 1995, *ApJ*, 445, L157
- Menten, K. M. & van der Tak, F. F. S. 2004, *A&A*, 414, 289
- Morino, J.-I., Yamashita, T., Hasegawa, T. & Nakano, T. 1998, *Nature*, 393, 340

- Panagia, N. 1973, *AJ*, 78, 929
- Plambeck, R. L., Wright, M. C. H., Mundy, L. G. & Looney, L. W. 1995, *ApJ*, 455, L189
- Reid, M. J. & Menten, K. M. 1997, *ApJ*, 476, 327
- Reid, M. J. & Menten, K. M. 2003, in *Mass-losing pulsating stars and their circumstellar matter*, *Astrophysics and Space Science Library*, Vol. 283, eds. Y. Nakada, M. Honma and M. Seki. (Kluwer Academic Publishers, Dordrecht), p. 283
- Shuping, R. Y., Morris, M. & Bally, J. 2004, *ApJ*, 128, 363
- Thronson, H. A. et al. 1986, *AJ*, 91, 1350
- van der Tak, F. F. S. & Menten, K. M. 2005, *A&A*, 437, 947

Table 1. Star & Disk Model Parameters

Parameter	Units	Model A	Model B	Model C
Opacity source		H ⁻ free-free	H ⁻ free-free	p ⁺ /e ⁻ bremsstrahlung
Stellar Radius (R_*)	AU	4	4	0.25
Disk Temperature at R_* ..	K	4500	3000	8000
Disk Density at R_*	cm ⁻³	1×10^{14}	1×10^{14}	6×10^{10}
Disk Thickness	AU	25	25	6
Temperature power law index ..		-0.5	-0.33	+0.0
Density power law index ...		-2.0	-2.00	-2.0
Stellar Luminosity ...	L_\odot	3×10^5	5×10^4	1×10^4
Disk Mass...	M_\odot	3	3	...

Note. — p⁺/e⁻ Bremsstrahlung model assumes a constant electron temperature and is insensitive to the stellar radius; also while the ionized disk mass is $\ll 1 M_\odot$, it is possible to have a substantial neutral mass that does not contribute to the emission. Power law indexes are defined as $\propto r^{\text{index}}$.

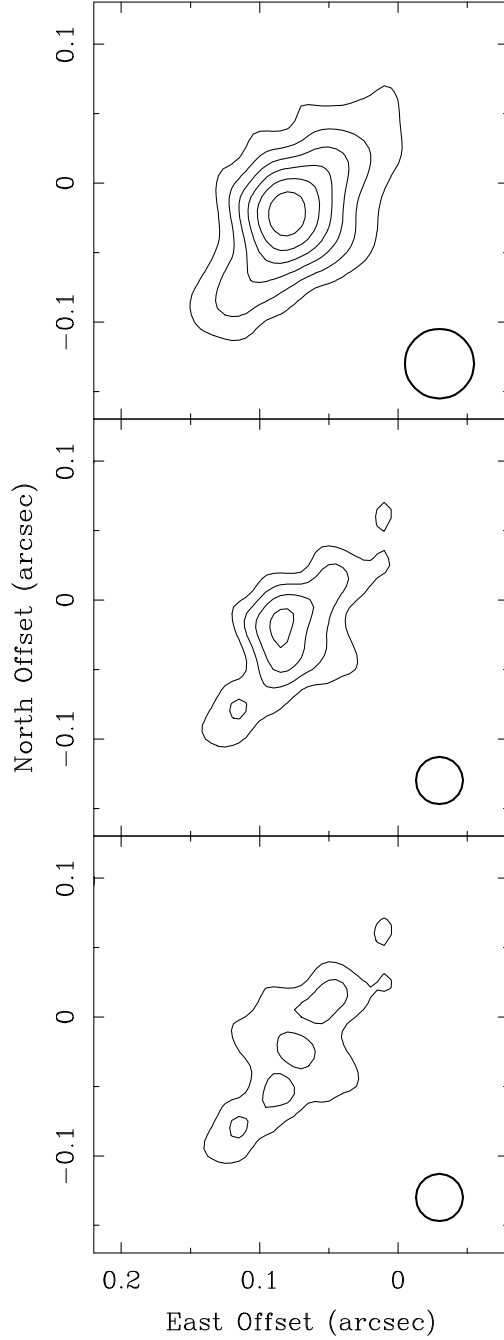


Fig. 1.— Continuum images of Orion-I at 43 GHz made with the VLA in the A-configuration. The image in the *upper panel* is at 50 mas (FWHM) resolution and the image in the *middle panel* is at 34 mas resolution. The emission is elongated NW–SE and may be from an disk surrounding a massive YSO. The brightest component near the center of the disk may be unresolved. When we subtract a point-like 2.2 mJy component from the (13 mJy total) emission, we obtain the image in the *lower panel*. In all images the contour levels are at integer multiples of 0.5 mJy beam^{−1}. The FWHM of the restoring beams are shown in the bottom right corner of each panel. At a distance of 480 pc, 0.1'' corresponds to 48 AU.

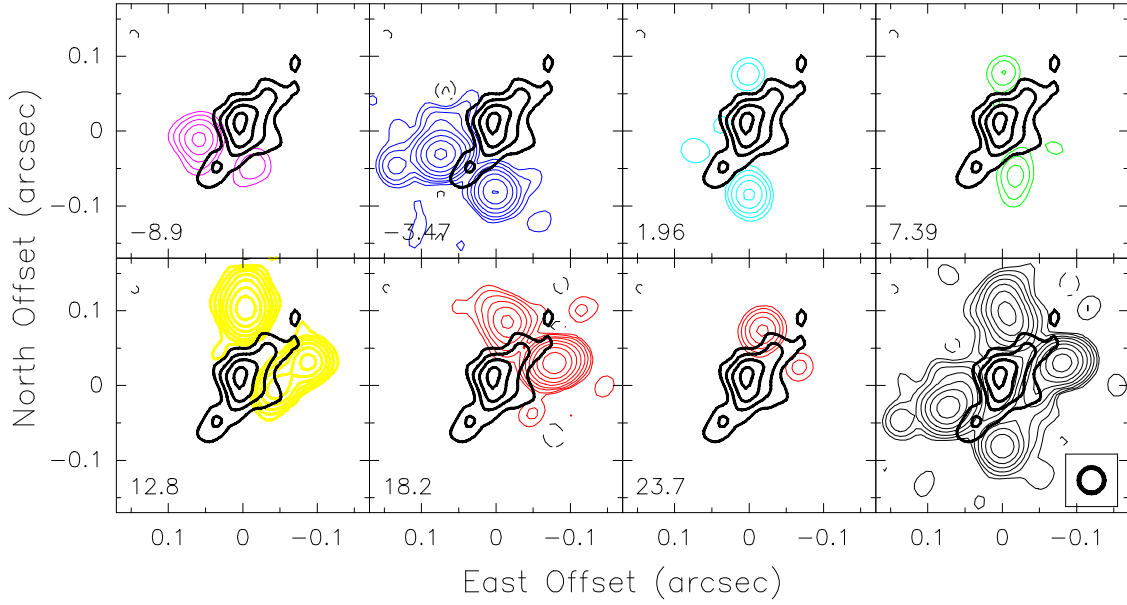


Fig. 2.— Orion-I SiO $v=1$, $J=1-0$ maser channel maps (*colored contours*) superposed on the 34 mas resolution continuum emission (*heavy black contours*). The colors are chosen to approximate those used in Fig. 1a of Greenhill et al. (1998); contouring levels start at 3 Jy beam^{-1} and increase by factors of 2. Center LSR velocities of the 5.43 km s^{-1} wide channels are given in the lower left corner of each panel. Continuum contours are integer multiples of $0.5 \text{ mJy beam}^{-1}$. The *bottom right panel* shows a map of the integrated SiO emission, with light contours at integer multiples of $0.18 \text{ Jy beam}^{-1} \text{ km s}^{-1}$. All position offsets are relative to Orion-I, whose position is $(\alpha, \delta)_{\text{J2000}} = (05^{\text{h}}35^{\text{m}}14.5121^{\text{s}}, -05^{\circ}22'0.521'')$ at 2000 Nov. 13 (Gómez et al. 2005).

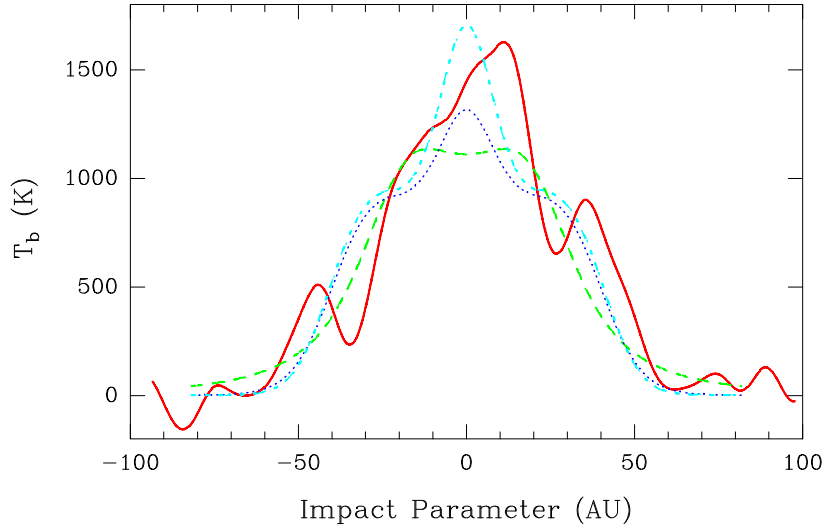


Fig. 3.— Brightness temperature profiles of the 43 GHz continuum emission of Orion-I. The observed profile (*solid red line*) is along the elongation of the edge-on disk-like emission in the 34 mas resolution image. Model profiles are shown for an edge-on disk with collisional ionization for central heating only (Model A, *blue dotted line*) and with additional local heating (Model B, *cyan dash-dotted line*; see §3.1). A photo-ionized disk model is also shown (Model C, *green dashed line*; see §3.2). Parameters for all models are listed in Table 1, and the model brightnesses have been convolved with a 34 mas Gaussian to approximate the observations.